Bioorganic & Medicinal Chemistry 16 (2008) 9975–9983

Contents lists available at ScienceDirect

Bioorganic & Medicinal Chemistry

journal homepage: www.elsevier.com/locate/bmc

Irreversible inhibition of dihydrodipicolinate synthase by 4-oxo-heptenedioic acid analogues

Berin A. Boughton [a,b], Michael D. W. Griffin [b,c], Paul A. O'Donnell [b], Renwick C. J. Dobson [b,c], Matthew A. Perugini [b,c], Juliet A. Gerrard [d], Craig A. Hutton [a,b,*]

[a] School of Chemistry, University of Melbourne, Parkville, Vic. 3010, Australia
[b] Bio21 Molecular Science and Biotechnology Institute, University of Melbourne, Parkville, Vic. 3010, Australia
[c] Department of Biochemistry and Molecular Biology, University of Melbourne, Parkville, Vic. 3010, Australia
[d] School of Biological Sciences, University of Canterbury, Christchurch, New Zealand

ARTICLE INFO

Article history:
Received 9 September 2008
Revised 10 October 2008
Accepted 11 October 2008
Available online 17 October 2008

Keywords:
Dihydrodipicolinate synthase
DHDPS
Enzyme inhibitors
Irreversible inhibition
Lysine biosynthesis

ABSTRACT

We report the synthesis of (2*E*,5*E*)-4-oxoheptadienedioic acid and (2*E*)-4-oxoheptenedioic acid and evaluation of both diester and diacid analogues as inhibitors of bacterial dihydrodipicolinate synthase. Enzyme kinetic studies allowed the determination of second-order rate constants of inactivation; and substrate co-incubation studies have shown the inhibitors act at the active-site. Mass spectrometric analyses have further explored the enzyme–inhibitor interaction and determined the sites of enzyme alkylation.

1. Introduction

Lysine (**8**) and its immediate precursor *meso*-diaminopimelate (*meso*-DAP, **7**), are essential elements of bacterial proteins and peptidoglycan.[1,2] As the biosynthetic pathway to lysine is only found in plants and bacteria, it has attracted considerable attention as a target for the design and synthesis of novel herbicides and antibiotics.[3–5]

The first committed step in the biosynthesis of lysine is the condensation of pyruvate (**1**) and aspartate semi-aldehyde (ASA, **3**), catalysed by the enzyme dihydrodipicolinate synthase (DHDPS) (Scheme 1).[6] Structural studies demonstrate that the active-site residues of DHDPS enzymes from all bacterial species characterised to date are highly conserved.[7] Initial condensation of the active-site lysine residue with pyruvate results in formation of a Schiff-base **2**.[8] Sodium borohydride trapping experiments have confirmed the initial reaction steps.[6,9] Tautomerisation and aldol-type reaction with ASA **3** then generates an enzyme-tethered acyclic intermediate **4** that undergoes transimination to form HTPA **5**, with concomitant release of the active-site lysine residue.[10] HTPA **5** is released from the active-site and elimination of water then provides dihydrodipicolinate (DHDP, **6**).

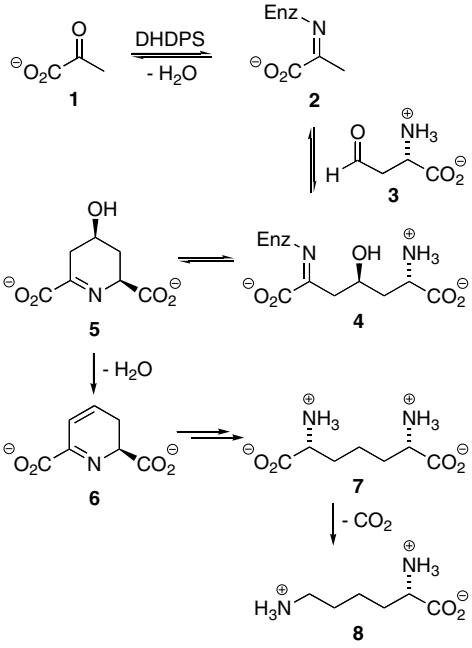

Scheme 1. The DHDPS catalysed condensation of pyruvate **1** and (*S*)-ASA **3** to form HTPA **5**, leading to eventual production of (*S*)-lysine **8**.

* Corresponding author. Tel.: +61 3 8344 2393; fax: +61 3 9347 8124.
E-mail address: chutton@unimelb.edu.au (C.A. Hutton).

0968-0896/$ - see front matter © 2008 Elsevier Ltd. All rights reserved.
doi:10.1016/j.bmc.2008.10.026

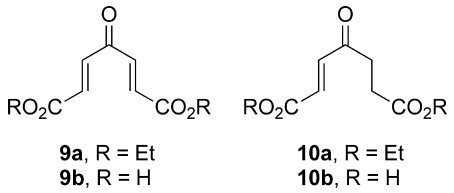

Figure 1. Structures of inhibitors **9a**, **9b**, **10a** and **10b**.

The design of inhibitors of DHDPS has traditionally been based upon substrate and product analogy.[8,11,12] Analogues of pyruvate have shown competitive inhibition with respect to pyruvate, including 3-fluoropyruvate (K_i = 0.22 mM), α-ketobutyrate (K_i = 0.83 mM), α-ketovalerate (K_i = 0.7 mM), glyoxylate (K_i = 0.016 mM),[13] and α,ε-diketopimelic acid (K_i = 0.16 mM).[14] α-Ketopimelic acid has been reported to be an irreversible inhibitor of DHDPS (K_i = 0.17 mM).[10] Product analogues have been designed to mimic the heterocycles DHDP (**6**) and HTPA (**5**),[11,15] but these inhibitors generally display poor inhibition of DHDPS, with inhibitory activity typically at low millimolar concentrations.

We have previously reported preliminary investigations into the synthesis and evaluation of two irreversible inhibitors of DHDPS, diethyl (2*E*,5*E*)-4-oxoheptadienedioate (**9a**) and diethyl (2*E*)-4-oxoheptenedioate (**10a**) (Fig. 1).[16] These compounds were designed to resemble the carbon framework and functionality of the enzyme-tethered acyclic intermediate **4**, while also possessing an electrophilic Michael acceptor to react with the active-site nucleophile.

In this full report, we describe the synthesis of the corresponding diacids, **9b** and **10b**, and thorough characterisation of the activity and mechanism of inactivation of DHDPS by all four of these inhibitors.

The four compounds have been designed to mimic the enzyme-tethered intermediate **4**, possessing a 7-carbon backbone with carboxylate functionality at either end and heteroatom functionality at the 4-position. They all possess an electrophilic unsaturated ketone group that can act as a Michael acceptor and thereby react with the active-site lysine ε-amino group. The diacids **9b** and **10b** more closely resemble the intermediate **4** than do the corresponding diesters **9a** and **10a**, and may engage in binding interactions, such as electrostatic interactions with the conserved arginine residue in the active-site of DHDPS. The dienes **9a** and **9b** could theoretically undergo two Michael-type to generate a lysine–piperidinone structure, whereas only a single Michael-type is possible with the alkenes **10a** and **10b**. Additionally, the dienes **9a** and **9b** are constrained in a rigid extended conformation by the (*E*,*E*)-stereochemistry of the double bonds and conjugation with the ketone group. In contrast, the alkenes **10a** and **10b** are expected to display greater conformational flexibility about the saturated C5–C7 section. Interestingly, diacid **9b** is reported as a moderate inhibitor of succinyl co-transferase (K_i^{app} = 0.53 mM),[4] another enzyme in the lysine biosynthetic pathway, and offers potential synergism via dual action.

2. Results

2.1. Synthesis of Inhibitors

Synthesis of the alkene and diene diesters, **9a** and **10a**, respectively, from diethyl 4-oxopimelate (**11**) was achieved by a bromination–elimination process (Scheme 2).[16]

Synthesis of the diacids, **9b** and **10b**, was initially attempted by base hydrolysis of the corresponding diesters **9a** and **10a**; however, these conditions resulted in the hydration of the double bonds to give mixtures of compounds including alcohols **15** and **12**, respectively. Alternative routes to the acids were therefore sought.

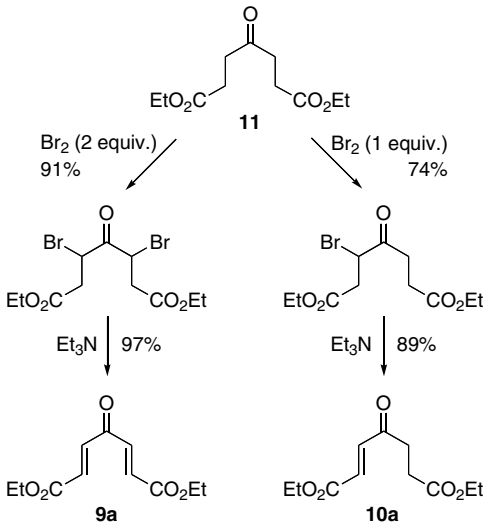

Scheme 2. Synthesis of **9a** and **10a** from diethyl 4-oxopimelate.

Diacid **10b** has previously been synthesised by partial hydrogenation of diene diacid **9a**[17] and bromination–oxidation of 2-furanpropionic acid.[18] However, we sought to overcome the problem of alkene hydration by performing hydrolysis of the ester **10a** under neutral conditions through simple reflux in distilled water.[19] This procedure initially gave the desired diacid **10b** and the corresponding hydrated compound **12** in a 1:2 ratio (Scheme 3). Treatment of the mixture in toluene at reflux overnight improved the ratio of **10b**:**12** to 3.5:1. Alkene **10b** and alcohol **12** were separated efficiently by trituration with water, which dissolved the more hydrophilic alcohol **12**, enabling isolation of the pure alkene **10b** in 40% yield. Further treatment of the isolated alcohol **12** in toluene at reflux gave more of the alkene **10b**.

The diene diacid **9b** was prepared using a modification of the procedure of Herman and Dreiding.[20] Aldol condensation of glyoxylic acid **13** and acetone dicarboxylic acid **14** gave the diol **15**. Dehydration of the diol **15** has been reported in refluxing toluene; however, we found that thermal dehydration of the solid diol **15** under reduced pressure gave **9b** in an improved yield (Scheme 4).

2.2. Enzyme kinetics

The inhibitory effect of these compounds against DHDPS was explored using a coupled assay with the next enzyme in the biosynthetic pathway, dihydrodipicolinate reductase (DHDPR), as pre-

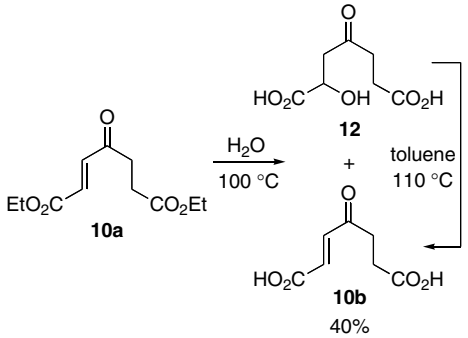

Scheme 3. Synthesis of **10b** by neutral hydrolysis of **10a**.

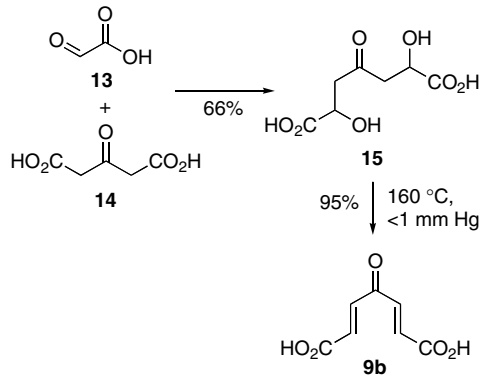

Scheme 4. Synthesis of **9b** by aldol reaction and thermal dehydration.

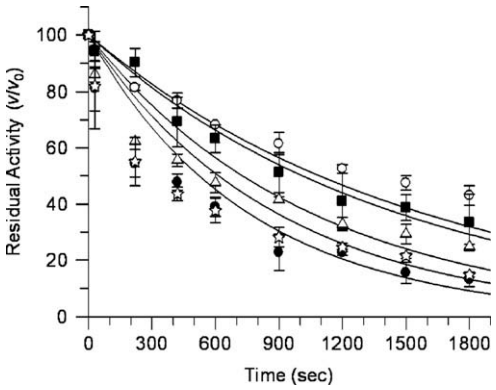

Figure 4. Residual activity of DHDPS upon incubation with **9b**; ○ = 0.5 mM, ■ = 1.2 mM, Δ = 2.0 mM, ● = 5.0 mM and ☆ = 10.0 mM.

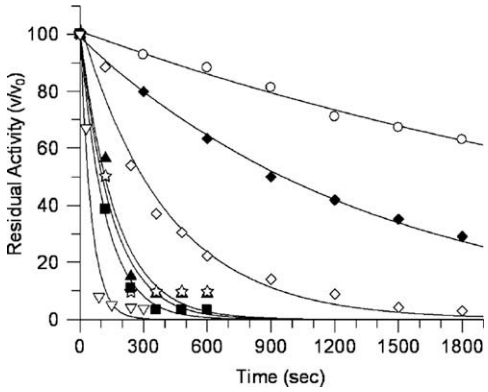

Figure 2. Residual activity of DHDPS upon incubation with **9a**; ○ = 0.125 mM, ♦ = 0.25 mM, ◇ = 0.5 mM, ▲ = 1.2 mM, ☆ = 1.5 mM, ■ = 2.0 mM, and ▽ = 10.0 mM.

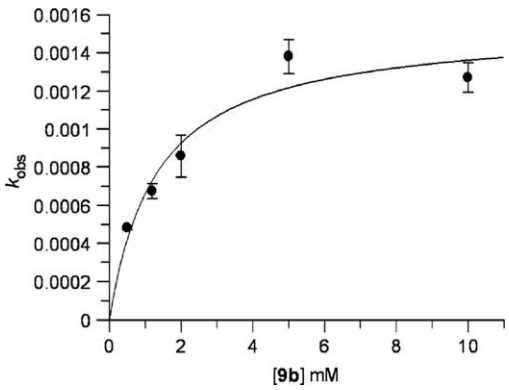

Figure 5. Plot of k_{obs} (rate of inactivation of enzyme, s^{-1}) versus [**9b**] (mM).

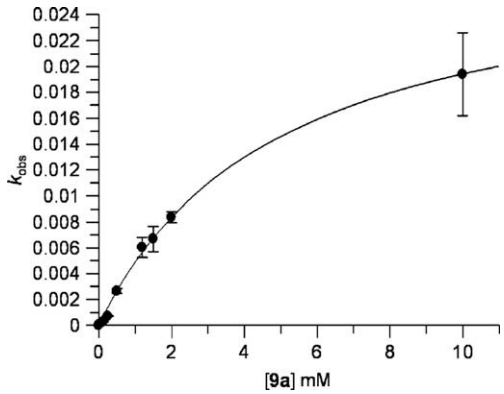

Figure 3. Plot of k_{obs} (rate of inactivation of enzyme, s^{-1}) versus [**9a**] (mM).

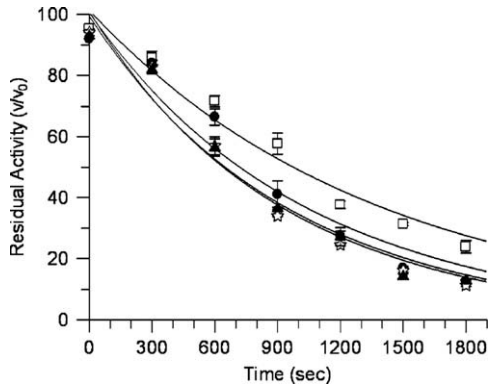

Figure 6. Residual activity of DHDPS upon incubation with **10a**; □ = 20 mM, ● = 50 mM, ☆ = 100 mM and ▲ = 250 mM.

viously described.[12,13] Detailed kinetics of time-dependent inhibition were determined using a modified coupled assay, wherein DHDPS was pre-incubated with the inhibitors for various time intervals prior to measuring activity.[16]

All compounds were found to inhibit DHDPS in a time-dependent manner (Figs. 2–9). Moreover, extensive dialysis of inhibited samples did not restore activity, indicating irreversible inactivation of the enzyme. The diene diester **9a** was found to be the most potent inhibitor, with complete inactivation of the enzyme within 6 min at 2 mM (Fig. 2). Analysis of the rate of enzyme inactivation over an inhibitor concentration range of 0.125–10 mM enabled determination of k_{inact}, K_i^{app}, and the second-order rate constant of inactivation, k_{inact}/K_i^{app} (5.9 M^{-1} s^{-1}, Table 1).[21] The diene diacid **9b** displayed moderate inhibition of DHDPS, with extended incubation at a concentration of 10 mM leading to almost complete loss of activity, corresponding to a second-order rate constant of 1.2 M^{-1} s^{-1} (Figs. 4 and 5 and Table 1). The K_i^{app} of the diacid **9b** was threefold lower than that of the diester **9a** (1.63 mM cf. 4.95 mM), suggesting tighter binding of the diacid, but the rate of inactivation once bound, k_{inact}, was considerably lower than that of the diester (0.0019 s^{-1} cf. 0.029 s^{-1}).

The mono-alkene inhibitors, diester **10a** and diacid **10b**, both displayed poor inhibition of DHDPS. The diester **10a** inhibited the enzyme with a second-order rate constant of 0.11 M^{-1} s^{-1}, and the analogous diacid **10b**, 0.12 M^{-1} s^{-1} (Figs. 6–9 and Table 1).

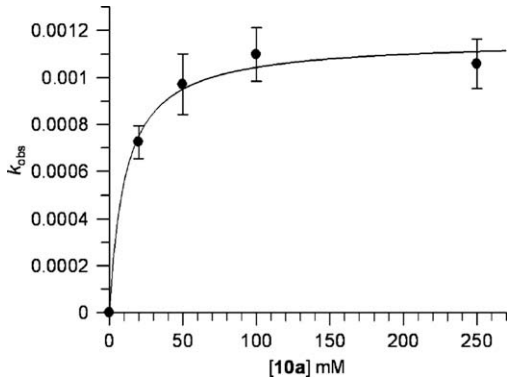

Figure 7. Plot of k_{obs} (rate of inactivation of enzyme, s^{-1}) versus [**10a**] (mM).

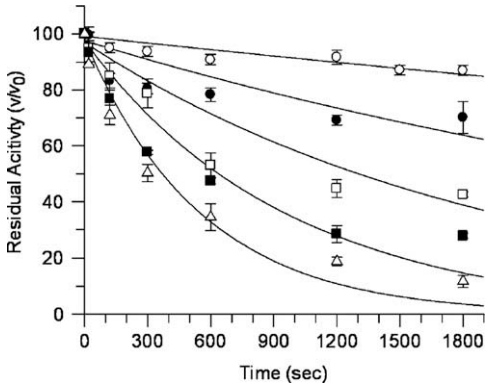

Figure 8. Residual activity of DHDPS upon incubation with **10b**; ○ = 0.1 mM, ● = 1.0 mM, □ = 5.0 mM, ■ = 10.0 mM and Δ = 25.0 mM.

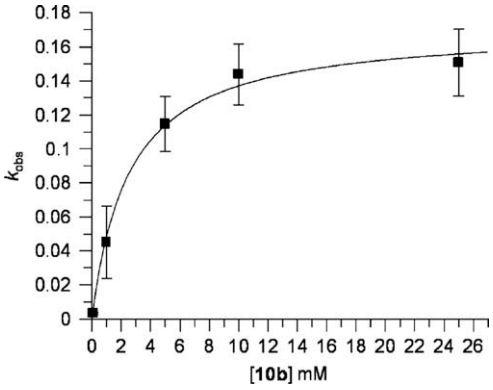

Figure 9. Plot of k_{obs} (rate of inactivation of enzyme, s^{-1}) versus [**10b**] (mM).

Table 1
Inhibition values for irreversible inhibitors **9a**, **9b**, **10a** and **10b**

Inhibitor	k_{inact} (s^{-1}, × 10^{-3})	K_i^{app} (mM)	R^2	k_{inact}/K_i^{app} (M^{-1} s^{-1})
9a	29.0 ± 1.1	4.95 ± 0.37	0.99	5.9
9b	1.9 ± 0.2	1.63 ± 0.46	0.95	1.2
10a	1.2 ± 0.05	10.9 ± 2.5	0.99	0.11
10b	4.1 ± 0.8	32.4 ± 9.8	0.97	0.12

Both the diester **10a** and diacid **10b** display high K_i^{app} values (>10 mM), indicative of poor binding to the active-site. This may be attributed to their inherent flexibility, thereby requiring a significant entropic cost in order to bind the active-site in a thermodynamically favourable conformation. Furthermore, dieneones are known to be more reactive than enones with regard to nucleophilic addition,[22] which may also account for the greater inhibitory activity of **9a** and **b** compared with **10a** and **b**. The inhibitors presumably exert their effect through covalent attachment to the active-site lysine by Michael-type addition of the lysine ε-amino group, as depicted in Scheme 5.

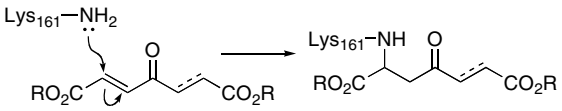

Scheme 5. Mechanism of inactivation of DHDPS.

2.3. Substrate protection of enzyme activity

In order to confirm that the inhibitors **9a** and **b** and **10a** and **b** bind at the active-site, substrate protection experiments involving co-incubation of DHDPS with each inhibitor and pyruvate (**1**) were performed (Fig. 10). Incubation of DHDPS with each of the inhibitors at high concentrations (⩾10 mM) resulted in rapid loss of activity. Incubation of DHDPS with each of the inhibitors in the presence of pyruvate (10 mM) resulted in negligible loss of activity, consistent with the mode of action of the inhibitors involving modification of the active-site lysine residue.

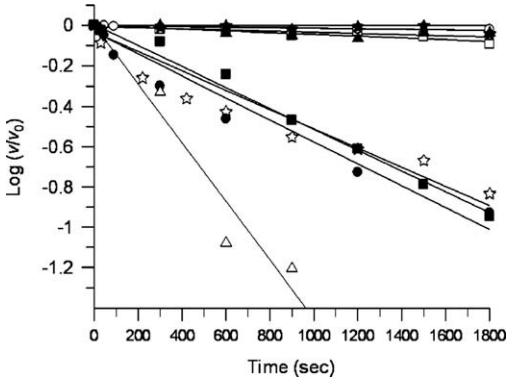

Figure 10. Plot showing pyruvate protection of enzyme inactivation; ▲ = 20 mM **9a** + 10 mM Pyr, □ = 10 mM **9b** + 10 mM Pyr, ★ = 100 mM **10a** + 10 mM Pyr, ○ = 25 mM **10b** + 10 mM Pyr, Δ = 20 mM **9a**, ☆ = 10 mM **9b**, ■ = 100 mM **10a**, ● = 25 mM **10b**.

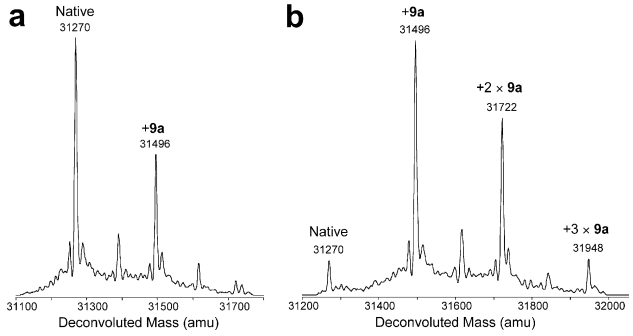

Figure 11. Mass spectra of DHDPS co-incubated with **9a** at; (a) t = 1 min and (b) t = 30 min.

2.4. Analysis of enzyme–inhibitor adducts

In order to confirm covalent attachment of the inhibitors to the enzyme, electrospray ionisation time-of-flight mass spectrometry (ESI-TOF-MS) experiments were performed. DHDPS was incubated with each of the inhibitors over a period of 30 min and aliquots analysed at 1 min, 5 min, and further 5-min intervals.

Following incubation of DHDPS with diene diester inhibitor **9a** for 1 min, native DHDPS ($[M+H]^+$, m/z = 31,270, where M = monomer of DHDPS) was observed along with an enzyme–inhibitor adduct ($[M+\mathbf{9a}+H]^+$, m/z = 31,496). An increase in fragmentation voltage led to no discernible difference in the observed spectra, demonstrating non-reversible covalent modification of the enzyme. After incubation for 30 min, adducts of DHDPS with multiple-inhibitor molecules were observed in the mass spectra. The major species were adducts of DHDPS with one or two inhibitor molecules, but trace amounts of adducts with 3–6 inhibitor molecules were also observed (Fig. 11).

A time-course analysis of the modification of DHDPS with **9a** via ESI-TOF-MS showed exponential decay of the native enzyme as it is modified with the irreversible inhibitor. The proportion of single-adduct (m/z = 31,496) increases rapidly until ~10 min, after which its abundance decreases slowly as multiple-inhibitor adducts form. The proportion of bis-adduct ($[M+2\times\mathbf{9a}+H]^+$, m/z = 31,722) slowly increases in abundance over the course of the experiment, while higher-order adducts (e.g. ($[M+3\times\mathbf{9a}+H]^+$, m/z = 31,948 and ($[M+4\times\mathbf{9a}+H]^+$, m/z = 32,174) are only present in trace amounts, even after 30 min (Fig. 12).

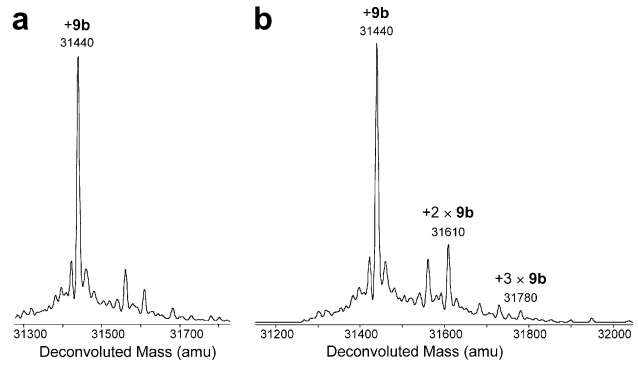

Figure 14. Mass spectra of DHDPS co-incubated with **9b** at; (a) t = 1 min and (b) t = 30 min.

The alkene diester **10a** (at 20 mM) displayed a similar profile upon incubation with DHDPS as the diene diester **9a** (at 0.5 mM). Time-course analysis again shows exponential decay of native DHDPS with rapid formation of the single-inhibitor adduct and slow formation of the bis-adduct. At t = 30 min the single-adduct was the major component, with a minor amount of the bis-adduct and trace amounts of higher-order adducts (Fig. 13).

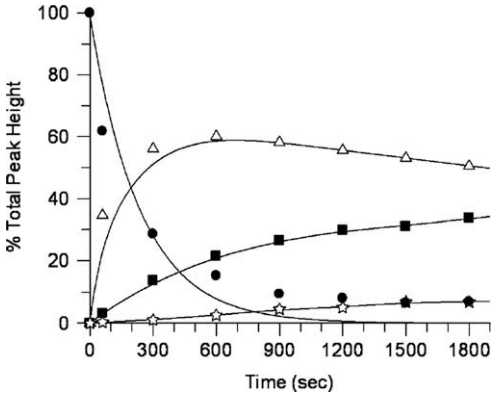

Figure 12. Composition of enzyme–inhibitor adducts upon incubation of DHDPS with **9a** [0.5 mM]; ● = native DHDPS, Δ = DHDPS + **9a**, ■ = DHDPS + 2 × **9a**, ☆ = DHDPS + 3 × **9a**.

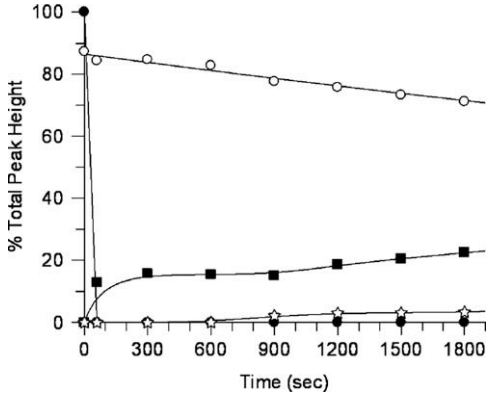

Figure 15. Composition of enzyme–inhibitor adducts upon incubation of DHDPS with **9b** (10 mM); ● = native DHDPS, ○ = DHDPS + **9b**, ■ = DHDPS + 2 × **9b**, ☆ = DHDPS + 3 × **9b**.

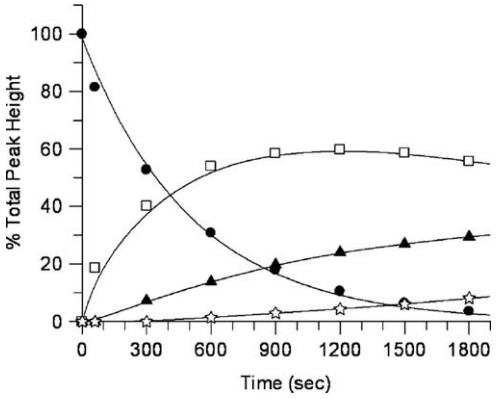

Figure 13. Composition of enzyme–inhibitor adducts upon incubation of DHDPS with **10a** [20 mM]; ● = native DHDPS, □ = DHDPS + **10a**, ▲ = DHDPS + 2 × **10a**, ☆ = DHDPS + 3 × **10a**.

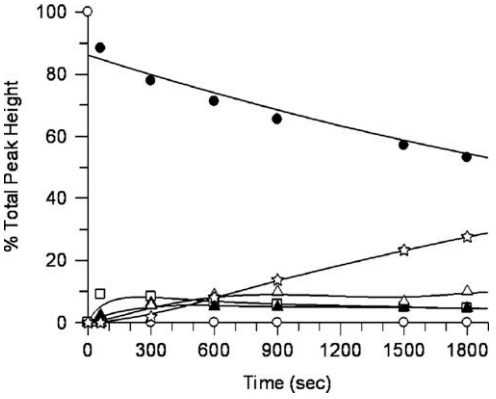

Figure 16. Composition of enzyme–inhibitor adducts upon incubation of DHDPS with **10b** (20 mM); ○ = native DHDPS, ● = DHDPS + **10b**, □ = DHDPS + 2 × **10b**, ▲ = DHDPS + 3 × **10b**, Δ = DHDPS + 4 × **10b**, ☆ = DHDPS + 5 × **10b**.

The diacids **9b** and **10b** exhibit a markedly different profile upon incubation with DHDPS than the corresponding diesters. Both **9b** and **10b** exhibit very rapid formation of a single-inhibitor adduct, with virtually no native DHDPS remaining after 1 min. Slow decay of the single-inhibitor adducts were then observed, as higher-order adducts are formed. Subsequent to formation of the single-adduct ($[M+\mathbf{9b}+H]^+$, $m/z = 31{,}440$), diene diacid **9b** shows slow addition of a second inhibitor molecule ($[M+2\times\mathbf{9b}+H]^+$, $m/z = 31{,}610$), with trace amounts of higher-order adducts (e.g. ($[M+3\times\mathbf{9b}+H]^+$, $m/z = 31{,}780$) again observed after long incubation times (Figs. 14 and 15).

Analysis of the incubation of DHDPS with mono-ene diacid **10b** shows that subsequent to the initial single-adduct formed, extended incubation results in slow decay of the single-adduct and accumulation of an adduct with five inhibitor molecules bound (Fig. 16). This result is in contrast to the other three inhibitors, which all show only trace amounts of higher-order adducts after extended incubation.

The rapid formation of the initial DHDPS–inhibitor adducts with diacid inhibitors **9b** and **10b** is presumably not due to alkylation at the active-site, as loss of DHDPS activity occurs much more slowly. The initial adduct from the diacid inhibitors is therefore likely to arise through alkylation of a surface nucleophilic residue, with alkylation of the active-site residue (and concomitant loss of activity) likely to correspond to the second alkylation process. In the case of the diester inhibitors, **9a** and **10a**, loss of enzyme activity does correlate with the rate of formation of the initial adduct, suggesting that initial alkylation of the active-site lysine residue is followed by alkylation of a nucleophilic surface residue. Evidence for the sites of alkylation and for the variation in reactivity of the inhibitors was sought through further mass spectrometric analyses, including trypsin digestion experiments.

2.5. Site(s) of covalent attachment of inhibitors

Mass spectrometric analysis of the incubation of DHDPS with pyruvate **1** confirmed formation of the Schiff-base **2**, as shown by conversion of native DHDPS ($m/z = 31{,}270$) to an adduct at $m/z = 31{,}340$ consistent with addition of pyruvate and loss of water (Fig. 17a).[9] Increasing the fragmentation voltage led to an increase in the proportion of the parent enzyme and a decrease in that of the adduct (data not shown), indicating reversal of pyruvate–adduct formation within the mass spectrometer. Incubation of DHDPS with pyruvate and diene diacid **9b** resulted in formation of the DHDPS–**9b** adduct ($m/z = 31{,}440$) and a DHDPS–pyruvate–**9b** adduct ($[M+Pyr+\mathbf{9b}+H]^+$, $m/z = 31{,}510$) (Fig. 17b). No higher-order adducts were observed. This observation is consistent with

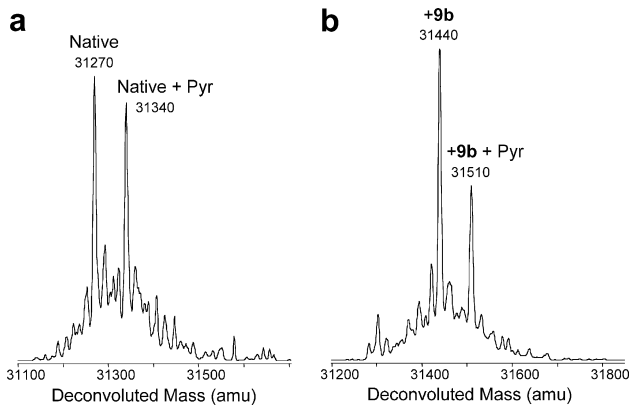

Figure 17. Mass spectra of DHDPS incubated with; (a) pyruvate (Pyr) and (b) pyruvate + **9b**.

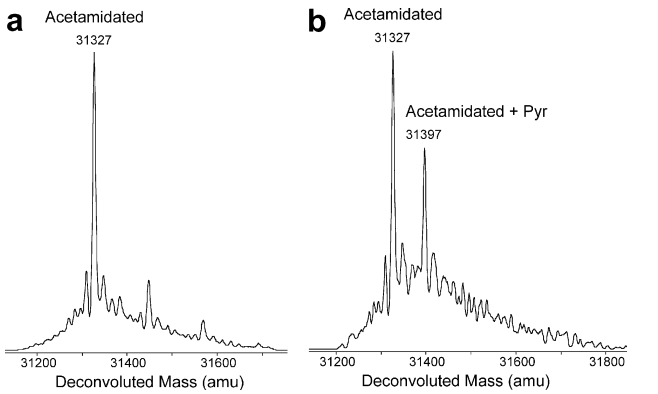

Figure 18. Mass spectra of; (a) DHDPS incubated with iodoacetamide, and (b) acetamidated DHDPS + pyruvate + **9b**.

pyruvate condensation with the active-site lysine residue and covalent attachment of **9b** to a surface nucleophile on the enzyme. Similar results were found with inhibitors **9a**, **10a** and **10b** (data not shown).

The identity of the reactive surface residue was investigated. It was envisaged that under the assay conditions, cysteine sulfhydryl groups would be the most reactive nucleophiles, although lysine amino groups could also be alkylation sites. *Escherichia coli* DHDPS contains thirteen lysine residues and five cysteine residues as potential nucleophilic sites. The ε-amino groups of eleven lysine residues and the sulfhydryl groups of two cysteine residues (Cys141 and Cys20) are visible on the surface of the enzyme, though solvent accessibility calculations using MolMol with a solvent radius of 1.4 Å suggest that the sulfhydryl group of just one cysteine residue, Cys20, is solvent accessible.

Direct confirmation of the site(s) of alkylation through tryptic digestion analysis of the DHDPS–pyruvate–**10b** adduct was unsuccessful. Accordingly, indirect evidence was sought by treating DHDPS with iodoacetamide, which is a known cysteine-specific reagent.[23,24] Following incubation with iodoacetamide, a mass shift of 57 Da to $m/z = 31{,}327$ was observed (Fig. 18a), consistent with alkylation of a single cysteine residue. Incubation of the acetamidated enzyme with pyruvate **1** resulted in a mass shift of 70 Da to $m/z = 31{,}397$ (Fig. 18b). This observation is consistent with the formation of the Schiff-base between pyruvate and the active-site lysine residue. Incubations of the acetamide-modified enzyme with pyruvate **1** and each inhibitors **9a**, **9b**, **10a** and **10b** showed there to be no further additions, indicating that each of the inhibitors reacts with the same surface nucleophile as iodoacetamide.

Attempted isolation of a single-inhibitor adduct of DHDPS with each of **10a** and **10b**, through quenching of incubations at $t = 1$ min, was unsuccessful. Further studies to determine the site(s) of alkylation were conducted using mono-ene diacid **10b**, with extended (12 h) incubation of DHDPS and **10b** conducted to ensure full conversion to the $+5\times$ **10b** adduct. Following dialysis, trypsin and chymotrypsin digests were performed and the digests analysed by MS/MS. Sequencing of the peptide fragments indicated that modifications were present on Cys218, Cys20, Cys256, Cys100, Cys141 and Lys161 (Table 2).

These results confirm covalent attachment of the inhibitor to the active-site lysine residue, Lys161. Further alkylations that give rise to the higher-order adducts must therefore occur on cysteine residues, with no evidence for alkylation of surface lysine residues.

Intriguingly, covalent adducts of each of the five cysteines with **10b** are detected, though the crystal structure of *E. coli* DHDPS shows only the sulfhydryl groups of residues Cys20 and Cys141 as being visible on the surface (Fig. 19). The carbonyl group of

Table 2
Major modified peptide fragments observed from trypsin or chymotrypsin digests of DHDPS incubated with **10b**

Entry	Digestion enzyme	Start	Amino acid sequence	Charge	Score	SPI
1	Chymotrypsin	198	(L)GGHGVISTANVAARDMAQM**c**KL(A)	4+	20.11	91.1
2	Trypsin	1	(−)MFTGSIVAIVTPMDEKGNV**c**R(A)	2+	20.20	89.5
3	Trypsin	254	(K)WA**c**KELGLVATDTLR(I)	2+	17.45	81.3
4	Chymotrypsin	81	(L)TQRFNDSGIVG**c**L(T)	2+	16.25	87.7
5	Chymotrypsin	152	(L)AKVK**n**IIGI**k**EATGNLTRVNQIKEL(V)	5+	15.69	70.5
6	Trypsin	121	(K)AIAEHTDLPQILYNVPSRTG**c**DLLPETVGR(L)	4+	15.49	74.8

'**c**' and '**k**' represent Cys and Lys residues, respectively, modified with **10b**. '**n**' denotes deamidation of arginine.

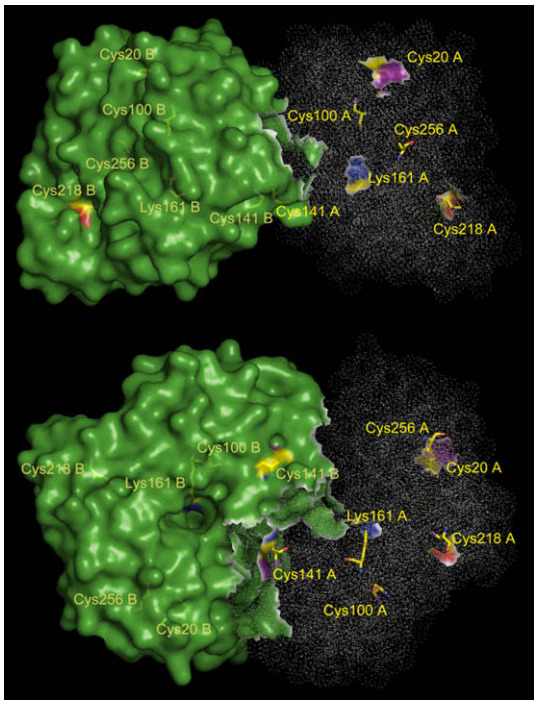

Figure 19. Surface analysis of DHDPS (C and D chains omitted for clarity. Yellow, C; blue, N; red, O; magenta, S). Top; view showing Cys20A sulfhydryl, Lys161A ε-amino group and Cys218A/B carbonyl on surface. Bottom; view looking into active-site cavity (chain B) and showing Cys141A/B partially on surface.

Cys218 is on the surface, and rotation of the Cα–Cβ bond would project the sulfhydryl group to the surface of the enzyme. Cys256 is within the C-terminal domain, on helix α10, which may be conformationally mobile with respect to the main αβ-barrel domain; such motion may render Cys256 surface-accessible.[25] Cys100 appears directed into the core of the enzyme, and it is not clear how the sulfhydryl group of this residue would be surface-accessible.

Presumably, in solution there is sufficient conformational mobility for these cysteine sulfhydryl groups, in addition to the active-site lysine ε-amino group, to access solvent and react with the electrophilic inhibitor **10b**.[26] The rapid formation of the bis-adduct presumably involves alkylation of Lys161 and the most-accessible cysteine residue (Cys20 or Cys141), with slower formation of higher-order adducts consistent with lower surface accessibility of the other cysteine residues.

3. Conclusion

We have demonstrated that this class of Michael acceptor is capable of irreversible inhibition of DHDPS. The diene inhibitors, **9a** and **9b**, are more potent than the corresponding mono-enes, **10a** and **10b**, with the diene diester **9a** being the best inhibitor of DHDPS in this series (highest k_{inact} and k_{inact}/K_i^{app} values). Mass spectrometry and tryptic digest analysis revealed that these inhibitors alkylate the active-site lysine residue (Lys161) and a surface cysteine residue, and more slowly alkylate other cysteine residues with lower surface accessibility. Intriguingly, co-incubation of DHDPS with the inhibitors in the presence of the substrate, pyruvate, not only protects against active-site alkylation, but also all but one of the cysteine residues. This result suggests that the conformational flexibility of the enzyme is substantially decreased in the presence of pyruvate.[27] While restriction of conformational freedom in enzyme–substrate complexes is a well-known phenomenon,[28] we are unaware of demonstration of this effect through modulation of reactivity of enzyme surface residues.

4. Experimental

4.1. Materials

Unless otherwise stated, all chemicals were purchased from Sigma–Aldrich or Novabiochem. Solvents and reagents were purified by the methods of Perrin and Armarego.[29] The compounds **9a** and **10a** were synthesized as previously reported.[16] (*S*)-ASA (**3**) was synthesized as previously described.[30] Enzymes were manipulated at 4 °C, or on ice and stored in Tris·HCl buffer (20 mM, pH 8.0 at 4 °C) at −20 °C. Protein concentration was measured using the method of Bradford.[31] Recombinant *E. coli* DHDPS and *E. coli* DHDPR were over-expressed and purified using the methods of Dobson et al.[32]

4.2. Methods

^{1}H NMR were collected on a Unity-VARIAN 400 MHz or 500 MHz NMR with either DMSO-d_6 (δ 2.49) or acetone-d_6 (δ 2.05) as internal standard. ^{13}C NMR are reported as parts per million (ppm) downfield shift with either DMSO-d_6 (δ 39.51) or acetone-d_6 (δ 206.26 (CO) and 29.84 (CD_3)) used as internal standard unless otherwise stated. HRMS were collected on a Finnigan LTQ-FT. Melting points were determined on a Gallenkamp Melting Point Apparatus. IR spectra were collected on a Bio-Rad FTS 165 FT-IR Spectrometer. Modeling was performed using MolMol or PyMOL with the published structure PDB 1YXC.[33] Surface exposure was calculated using MolMol with a solvent radius of 1.4 Å.

4.3. Synthesis

4.3.1. 4-Oxo-2,6-dihydroxyheptandioic acid (15)[20]

To 1,3-acetonedicarboxylic acid (**14**) (20.47 g, 140 mmol) in H_2O (100 mL) was added glyoxylic acid (**13**) (20.49 g, 277 mmol) and pyridine (200 μL). The resulting mixture was stirred for 3 days after which it was heated to 50 °C for 1 h. The mixture was then dried in vacuo to yield a yellow oil, which crystallized on standing to give the diol **15** as an amorphous off-white powder (19.0 g, 66%); mp 143–144 °C, (lit.[20] mp 155–157 °C). ^{1}H NMR (300 MHz,

D_2O): δ 4.41 (m, 2H), 2.91 (m, 2H), 2.85 (m, 2H). ^{13}C NMR (100 MHz, DMSO-d_6): δ 205.1, 174.9, 66.0, 47.0. IR (υ_{max}, cm^{-1}): 3408 br, 2965 br, 2921, 2624 br, 1725, 1448, 1390, 1266, 1251, 1241, 1113, 893. HRMS-ESI (m/z): calculated for $C_7H_9O_7^-$ 205.0343; found 205.0347 $[M-H]^-$.

4.3.2. (*E*,*E*)-4-Oxo-hept-2,5-dienedioic acid (9b)[20]

4-Oxo-2,6-dihydroxyheptandioic acid (**15**) (332 mg, 1.61 mmol) was heated (160 °C) under vacuum (<1 mmHg) for 16 h to give a fine brown powder which was used without further purification (260 mg, 95% yield); mp 195–200 °C (lit.[20] mp 243–245 °C). ^1H NMR (DMSO-d_6, 400 MHz): δ 7.25 (d, 2H, J = 15.6 Hz), 6.68 (d, 2H, J = 15.6 Hz). ^{13}C NMR (DMSO-d_6, 100 MHz): δ 189.1, 166.2, 137.5, 133.4. IR (υ_{max}, cm^{-1}): 2950 br, 1683, 1404, 1204. HRMS-ESI (m/z): calculated for $C_7H_5O_5^-$ 169.0132; found 169.0135 $[M-H]^-$.

4.3.3. (*E*)-4-Oxo-2-heptendioic acid (10b)[18]

Diethyl 4-oxo-2-hept-(*E*)-endioate (**10a**) (500 mg, 2.19 mmol) was heated at reflux in H_2O for 12 h. The reaction mixture was washed with CH_2Cl_2 (30 mL), then concentrated in vacuo to yield a 1:2 mixture of **10a** and **12** as a tan solid (249 mg). The solid was dissolved in a minimum of water and transferred to a Dean-Stark apparatus. Toluene (5 mL) was added and the mixture heated at reflux overnight. The toluene was removed in vacuo to give a brown solid (201 mg), which was triturated with water, filtered, rinsed with cold water and dried to give the pure alkene **10b** as a white solid (152 mg, 40%); mp 183–184 °C, (lit.[18] mp 186 °C). ^1H NMR (400 MHz, acteone-d_6): δ 7.03 (d, 1H, J = 16.2 Hz), 6.71 (d, 1H, J = 16.2 Hz), 3.04 (t, 2H, J = 6.4 Hz), 2.62 (t, 2H, J = 6.4 Hz). ^{13}C NMR (100 MHz, acetone-d_6): δ 199.6, 174.5, 167.4, 141.1, 132.3, 37.1, 28.6. IR (υ_{max}, cm^{-1}): 2877 br, 1686, 1667, 1626, 1431, 1402, 1251, 1162, 928. HRMS-ESI (m/z): calculated for $C_7H_7O_5^-$ 171.0299; found 171.0291 $[M-H]^-$.

4.4. Assay for monitoring DHDPS activity

UV–vis spectra and kinetic data were collected on either a Hewlett Packard 8452A Diode Array spectrophotometer with a circulating water bath to maintain a constant temperature of 30 °C or a Cary 50 Bio UV–vis Spectrophotometer equipped with a Haake P5/DC10 circulating water bath to maintain a constant temperature of 30 °C. The concentration of (*S*)-ASA (**3**) was determined as previously described.[12] Modified assay conditions were utilized to determine rates of inactivation of irreversible inhibitors.[16] Substrate protection experiments were conducted by incubating DHDPS with inhibitor and pyruvate (**1**) (10 mM).

4.5. Analysis of enzyme kinetics data

Results were analysed by the methods of Copeland,[34] where the observed decay curve for each concentration of inhibitor was fitted to Eq. (1), to determine k_{obs}. A plot of k_{obs} versus [I], was fitted to Eq. (2) to determine values for k_{inact} and K_i^{app}. The second-order rate constants of irreversible enzyme inhibition were then derived by determining k_{inact}/K_i^{app}.

$$\frac{v}{v_0} = e^{(-k_{obs} \times t)} \quad (1)$$

$$k_{obs} = \frac{(k_{inact} \times I)}{(K_i^{app} + I)} \quad (2)$$

4.6. Preparation of modified DHDPS

Native *E. coli* DHDPS (~2.0 mg mL^{-1} in Tris·HCl (20 mM), pH 8.0 at 25 °C) used in digestion experiments was modified by incubation with a solution of **10b** (100 mM in Tris·HCl (100 mM), pH 8.0 at 25 °C). Incubation with pyruvate (**3**) was performed by addition of pyruvate (**1**) to a stock solution of DHDPS followed by immediate addition of inhibitor. Acetamidated DHDPS was prepared by incubation with iodoacetamide (5 mM) for 30 min at 25 °C, followed by dialysis of the sample, twice for 3 h each against Tris·HCl buffer (20 mM, pH 8.0 at 4 °C).[23]

4.7. Proteolytic digestion of DHDPS

Enzyme digestion was performed using either α-chymotrypsin or trypsin. The modified sample (50 μL was then dialysed (3 × 500 mL) against Tris·HCl ((100 mM), pH 7.8 at 25 °C). α-Chymotrypsin stocks were provided by suspension of lyophilised sequencing-grade enzyme in HCl (1 mM) and $CaCl_2$ (2 mM) buffer. Trypsin stocks were provided by suspension of modified sequencing-grade trypsin in HCl (1 mM). Digestion was initiated by the addition of either α-chymotrypsin or trypsin solution to DHDPS solution to give a ratio of α-chymotrypsin or trypsin:DHDPS of 1:20. Digestion using α-chymotrypsin was performed in Tris·HCl (100 mM, pH 7.4) and $CaCl_2$ (10 mM), 5% acetonitrile buffer at 25 °C overnight. Trypsin digestions were performed in Tris·HCl (100 mM), pH 8.0 at 25 °C, 5% trifluoroethanol and 15% acetonitrile buffer for a minimum of 16 h.

4.8. Mass spectrometry

ESI-TOF-MS were performed on either an Agilent LC/MSD TOF mass spectrometer or an Agilent 6510 Q-TOF LC/MS mass spectrometer each coupled to an Agilent 1100 LC system (Agilent, Palo Alto, CA). Time dependent experiments were performed by addition of inhibitor to a stock solution of enzyme in Tris·HCl (20 mM, pH 8.0 at 25 °C) buffer; aliquots were taken at t = 1 min, 5 min, then at 5 min intervals until 30 min.

ESI-MS/MS sequencing was performed using an Agilent 6510 Q-TOF LC/MS mass spectrometer equipped with a Agilent 1100 LC system and Agilent Eclipse C18 reverse phase 5 μm, 2.1 mm × 150 mm column. Samples were injected directly with 5% acetonitrile/0.1% formic acid at 250.0 μL min^{-1}. Peptides were eluted with a gradient of 5% acetonitrile/0.1% formic acid to 45% acetonitrile/0.1% formic acid over 40 min, followed by a 2-min step of 45–90% acetonitrile/0.1% formic acid to elute any remaining protein from the column.

Further LC-ESI-MS/MS experiments were performed using an Agilent 1100 Series HPLC coupled to an Agilent LC/MSD Trap XCT Plus mass spectrometer fitted with an HPLC chip cube (Agilent, Palo Alto, CA). The HPLC chip comprised a 40 nL enrichment column and a 75 μm × 43 mm separation column both packed with Zorbax 300SB—C18 5 μm material. Samples were loaded onto the enrichment column in 5% acetonitrile/0.1% formic acid at 4.0 μL min^{-1}. A 9 min linear gradient (flow rate 500 nL min^{-1}) from 5 to 60% acetonitrile/0.1% formic acid was performed followed by a 1 min step of 60–80% acetonitrile/0.1% formic acid over 0.5 min and held for 0.5 min to elute any remaining protein from the column.

4.9. Database search

A user database incorporating the known sequence of *E. coli* DHDPS[35] was searched using the Agilent Spectrum Mill Server software (Rev. A.03.02.). Peak lists were created with the Spectrum Mill Data Extractor program with the following attributes: scans with the same precursor ±1.4 m/z were merged within a time frame of ±30 s for Q-TOF data and ±15 s for Ion Trap data. Precursor ions needed to have a minimum signal to noise value of 30. Charges up to a maximum of +9 were assigned to the precursor ion, and the ^{12}C peak was determined by Data Extractor. The user

database was searched for tryptic or chymotryptic peptides with a mass tolerance of ±2.5 Da for the precursor ions and a tolerance of 0.7 Da for the fragment ions. Up to five missed cleavages were allowed. Variable modifications were allowed and included the possibilities of carbamidomethylation, oxidized methionine, deamidation and modification on lysine and cysteine of the **10b** inhibitor. Minimum scores and minimum scored peak intensity (SPI) were dependent on the assigned precursor charge. Manual validation of a combined library of peptides from each digest and data extraction was then performed in Protein Peptide/Summary mode. From a total of 6 digests and 21 separate LC–MS experiments of the modified enzyme with search settings limited to a minimum score of 15 and SPI $\geqslant$ 60, a library of 168 spectra with 42 peptides accounted for a sequence coverage of 90%. Lowering of the required score to 13 gave sequence coverage of 97% with SPI $\geqslant$ 60 and 279 spectra with 58 distinct peptides. Lowering of the SPI from the recommended 70–60 allowed for the possibility of unknown cleavages and fragmentations generated by the presence of a modified lysine or cysteine residue within the peptide. Substitutions of cysteine have been shown to significantly alter the backbone cleavage observed in CID experiments.[36] Similar analysis of the data derived from control digestions of the native enzyme gave a library of 189 spectra with 29 peptides, 82% sequence coverage with a minimum score of 15 and SPI $\geqslant$ 70. All protein hits found in a distinct database search by Spectrum Mill are non-redundant. To eliminate redundancy, the Protein Summary Mode groups all proteins that have at least one common peptide, and only the highest scoring member of each protein group is shown and counted in the protein list.

Acknowledgments

The authors thank F.G. Pearce for useful discussions and C. Baxter for surface accessibility calculations. The Australian Research Council (DP0770888 and LX0776388), Defense Threat Reduction Agency (Project ID AB07CBT004) and Royal Society of New Zealand Marsden Fund supported this work.

References and notes

1. Bukhari, A. I.; Taylor, A. L. *J. Bacteriol.* **1971**, *105*, 844.
2. Pavelka, M. S., Jr.; Jacobs, W. R., Jr. *J. Bacteriol.* **1996**, *178*, 6496.
3. Hutton, C. A.; Perugini, M. A.; Gerrard, J. A. *Mol. Biosyst.* **2007**, *3*, 458.
4. Cox, R. J.; Sutherland, A.; Vederas, J. C. *Bioorg. Med. Chem.* **2000**, *8*, 843.
5. Cox, R. J. *Nat. Prod. Rep.* **1996**, *13*, 29.
6. Shedlarski, J. G.; Gilvarg, C. *J. Biol. Chem.* **1970**, *245*, 1362.
7. Kefala, G.; Evans, G. L.; Griffin, M. D. W.; Devenish, S. R. A.; Pearce, F. G.; Perugini, M. A.; Gerrard, J. A.; Weiss, M. S.; Dobson, R. C. J. *Biochem. J.* **2008**, *411*, 351.
8. Hutton, C. A.; Southwood, T. J.; Turner, J. J. *Mini Rev. Med. Chem.* **2003**, *3*, 115.
9. Borthwick, E. B.; Connell, S. J.; Tudor, D. W.; Robins, D. J.; Shneier, A.; Abell, C.; Coggins, J. R. *Biochem. J.* **1995**, *305*, 521.
10. Blickling, S.; Renner, C.; Laber, B.; Pohlenz, H.-D.; Holak, T. A.; Huber, R. *Biochemistry* **1997**, *36*, 24.
11. Couper, L.; McKendrick, J. E.; Robins, D. J.; Chrystal, E. J. T. *Bioorg. Med. Chem. Lett.* **1994**, *4*, 2261.
12. Coulter, C. V.; Gerrard, J. A.; Kraunsoe, J. A. E.; Pratt, A. J. *Pestic. Sci.* **1999**, *55*, 887.
13. Karsten, W. E. *Biochemistry* **1997**, *36*, 1730.
14. Yamakura, F.; Ikeda, Y.; Kimura, K.; Sasakawa, T. *J. Biochem.* **1974**, *76*, 611.
15. Turner, J. J.; Gerrard, J. A.; Hutton, C. A. *Biorg. Med. Chem.* **2005**, *13*, 2133.
16. Turner, J. J.; Healy, J. P.; Dobson, R. C. J.; Gerrard, J. A.; Hutton, C. A. *Bioorg. Med. Chem. Lett.* **2005**, *15*, 995.
17. Igarashi, M. *J. Sci. Res. Inst.* **1957**, *51*, 82.
18. Koga, W. *Nippon Kagaku Kaishi, Pure Chem. Sect.* **1954**, *75*, 147.
19. Sunilkumar, G.; Nagamani, D.; Argade, N. P.; Ganesh, K. N. *Synthesis* **2003**, 2304.
20. Hermann, K.; Dreiding, A. S. *Helv. Chim. Acta* **1976**, *59*, 626.
21. The second-order rate constants of inactivation reported in Ref. 16 were calculated from the initial slope of the plot of k_{obs} versus [*I*]. We have now conducted assays over a greater range of [*I*] allowing determination of k_{inact}, K_i^{app}, and the second-order rate constant, k_{inact}/K_i^{app}. The values are in accordance with those reported in Ref. 16.
22. Suzuki, M.; Mori, M.; Niwa, T.; Hirata, R.; Furuta, K.; Ishikawa, T.; Noyori, R. *J. Am. Chem. Soc.* **1997**, *119*, 2376.
23. Jones, J. G.; Otieno, S.; Barnard, E. A.; Bhargava, A. K. *Biochemistry* **1975**, *14*, 2396.
24. De Vries, T.; Yen, T.-Y.; Joshi, R. K.; Storm, J.; Van den Eijnden, D. H.; Knegtel, R. M. A.; Bunschoten, H.; Joziasse, D. H.; Macher, B. A. *Glycobiology* **2001**, *11*, 423.
25. Mirwaldt, C.; Korndoerfer, I.; Huber, R. *J. Mol. Biol.* **1995**, *246*, 227.
26. Griffin, M. D. W.; Dobson, R. C. J.; Pearce, F. G.; Antonio, L.; Whitten, A. E.; Liew, C. K.; Mackay, J. P.; Trewhella, J.; Jameson, G. B.; Perugini, M. A.; Gerrard, J. A. *J. Mol. Biol.* **2008**, *380*, 691.
27. A substantial effect on the dynamics and inhibition of MosA, a DHDPS from *S. meliloti*, in the presence of pyruvate was recently reported: Phenix, C. P.; Palmer, D. R. J. *Biochemistry* **2008**, *47*, 7779.
28. (a) Fersht, A. *Structure and Mechanism in Protein Science: A Guide to Enzyme Catalysis and Protein Folding*, W.H. Freeman and Company, 1999.; (b) Stivers, J. T.; Abeygunawardana, C.; Mildvan, A. S.; Whitman, C. P. *Biochemistry* **1996**, *35*, 16036.
29. Armarego, W. L. F.; Perrin, D. D. *Purification of Laboratory Chemicals*, 4th ed.; Butterworth-Heinemann, 1997.
30. Roberts, S. J.; Morris, J. C.; Dobson, R. C. J.; Baxter, C. L.; Gerrard, J. A. *ARKIVOC* **2004**, 166.
31. Bradford, M. M. *Anal. Biochem.* **1976**, *72*, 248.
32. Dobson, R. C. J.; Gerrard, J. A.; Pearce, F. G. *Biochem. J.* **2004**, *377*, 757.
33. Dobson, R. C. J.; Griffin, M. D. W.; Jameson, G. B.; Gerrard, J. A. *Acta Cryst. D* **2005**, *D61*, 1116.
34. Copeland, R. A. *Enzymes: A Practical Introduction to Structure, Mechanism, and Data Analysis*, 2nd ed.; Wiley-VCH Inc., 2000.
35. Richaud, F.; Richaud, C.; Ratet, P.; Patte, J. C. *J. Bacteriol.* **1986**, *166*, 297.
36. Kapp, E. A.; Schuetz, F.; Reid, G. E.; Eddes, J. S.; Moritz, R. L.; O'Hair, R. A. J.; Speed, T. P.; Simpson, R. J. *Anal. Chem.* **2003**, *75*, 6251.